

Particle Size Dependent Gas Sensing Performance of ZnO Nanorods based Thick Film Resistors

Snehal D. Patil, Y. B. Patil, D. R. Patil*
Bulk and Nanomaterials Research Lab.,
Dept. of Physics, R. L. College, Parola,
Dist. Jalgaon, MHS, India, 425111

*E-mail: prof_drpatil@yahoo.in Mob: +91 9860335029

Shahera S. Patel
Dept. of Electronics,
Sardar Patel University,
V. V. Nagar, Gujarat, India, 388001

Abstract- Pure bulk ZnO was observed to be less sensitive to hazardous, toxic and inflammable gases. As the particle size of the materials get reduced from bulk to nanoscale, the gas sensing performance of pure ZnO was observed to increase crucially. It was also observed that, further decrease in the particle size would leads to decrease in the gas response. The optimized average diameter of ZnO Nanorod / particle size is 12 nm, which exhibits crucial gas response. The disc type ultrasonicated microwave assisted centrifuge technique was used for the synthesis of materials. The dry powders of synthesized materials were transformed into thick films by screen printing technique. Various characterizations techniques were employed to study the surface topography, crystal structure, phase, particle size, etc. effect of the surface nanostructure, different gases, gas concentrations, particle size, long duration for ageing, etc. on the gas response of the samples were studied and discussed.

Keywords: Bulk and nano ZnO, Thick films, Gas sensors, Particle size, Nanorods, etc

I. INTRODUCTION

There is a strong interest in the development of wide band gap semiconductor gas sensors for the applications including detection of fuel leak in spacecrafts, aircrafts, automobiles, fire detectors, exhaust diagnosis, emissions from industrial processes, etc. It was discovered in 1950, that the electrical properties of some metal oxides are changed [1] when they exposed to oxidizing or reducing gases. Seiyama et al [2] in 1962, proposed the idea of gas sensing using ZnO thin films. Taguchi [3] proposed that the SnO₂ acts as a gas sensor in the same year. Figaro engineering [4] fabricated and has made available these sensors for commercial use since 1968. Taguchi gas sensor was made from partially sintered SnO₂ bulk device whose resistance in air is very high and falls down when exposed to reducing gases and combustible gases (viz. H₂, CH₄, VOCs, etc). To study and develop the fundamentals of the gas sensing mechanism, the semiconducting sensors are modified by simple addition of metals (viz. Al, In, Cu, Sn, Fe, Ru, Pt, Pd, etc), in the base materials, which is referred as doping. Metal oxides such as ZnO, SnO₂, Fe₂O₃, TiO₂, WO₃, ZrO₂, etc. have also been used as gas sensors. Other than these broad studies for the semiconductor based gas sensors, few difficulties such as poor sensitivity, less selectivity, inability to detect the trace level of the gas (ppm/ppb) and minimization of the sensor performance due to surface contamination still persist. Thus, there is a growing need for gas sensors with novel properties. This can be achieved at nanoscale materials science.

The nanoscale science and technology are fuelling a new wave of revitalization in the field of gas sensors. The gas response of any metal oxide semiconductor to a particular gas increases with decrease in the size of grains / crystallites [5] due to increase in surface to volume ratio and

therefore the reactivity. Crystallite size and nanostructures of the sensor affect the sensing performance of the sensor. It was found that, the area of active surface sites is larger for smaller grain size of the sensor materials. This attributes to enhance the gas response and selectivity. Several recent research reports have confirmed the benefits of "nano-scaled materials" on sensor performance [6, 7]. The sensor showed good response by controlling its' particle size below 10-60 nm. It was also observed that the gas response was decreased with increasing the particle size on sintering at high temperature [8, 9]. Proper control of grain size remains a key challenge for high sensing performance.

As ammonia is extensively utilized in various fields [10], the leak in the system can result the health hazards. Ammonia is harmful and toxic [11-15]. Ammonia exposure causes lung diseases, irritating and burning the respiratory track. Environmental pollution [16-19] is a burning global issue; pollution has raised its ugly head high in the environment. Therefore, all industries working on and for ammonia should have an alarm system detecting and warning for dangerous ammonia concentrations. So, it is the need to fabricate and develop the ammonia sensor.

Some well-known materials for NH₃ gas sensing are modified-ZnO (viz. Fe-ZnO, Pd-ZnO, and Ru-ZnO) [20, 21], molybdenum oxide [22], polyaniline [23], polypyrrole [24], Au and MoO₃-modified WO₃ [25, 26], Pt and SiO₂-doped SnO₂ [27] etc. Few sensor models are also available for detecting ammonia gas. They are: Figaro gas sensor model - TGS 824 (detection range 300 ppm) and Sierra gas monitor model - CM 99-447 (electrochemical type, detection range 200 ppm). In the present work, efforts are made to develop the room temperature NH₃ gas sensor, using low cost and easily available materials.

II. EXPERIMENTAL

A. Synthesis of nano-ZnO powder

Nanostructured ZnO powder was synthesized by disc type ultrasonicated microwave assisted centrifuge technique. 0.50 M Zinc Nitrate (A. R. grade) alcoholic solution was prepared and ammonium hydroxide was added drop wise slowly with the constant stirring on hotplate, till precipitation obtained and pH reaches at 10.5. The ppt was washed out 6 times with de-ionized water. The ppt was allowed to ultrasonicated for 30 minutes followed by microwave irradiation and centrifugation. As prepared powder was calcined at 500°C for 2 hrs. Different samples were prepared by varying the concentrations of the precursors at various pH values and at other parameters. These samples were named as Z_b, Z₁, Z₂, and Z₃ depending on their crystallite size, respectively.

B. Thick film fabrication

The thixotropic paste [28-35] was formulated by mixing the synthesized nanostructured ZnO powder with a solution of ethyl cellulose (a temporary binder) in a mixture of organic solvents such as butyl cellulose, butyl carbitol acetate and turpineol. The ratio of inorganic to organic part was kept as 80: 20 in formulating the paste. The thixotropic paste was screen printed on a glass substrate in desired patterns. Films prepared were fired at 500°C for 30 min. Silver contacts were made by vacuum evaporation for electrical measurements.

C. Details of static gas sensing system

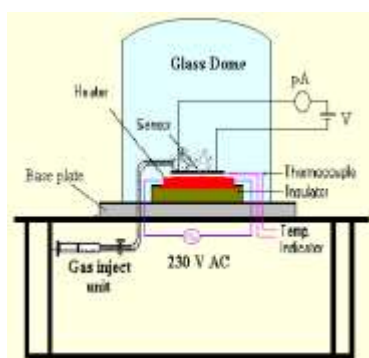


Fig. 1 Block diagram of static gas sensing system

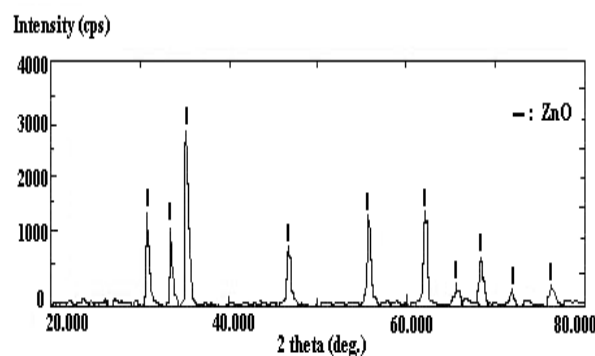
Fig. 1 represents 'static gas sensing system' to examine the sensing performance of the thick films. There were electrical feeds through the base plate. The heater was fixed on the base plate to heat the sample under test upto required operating temperature. The current passing through the heating element was monitored using a relay with adjustable ON and OFF time intervals. A Cr-Al thermocouple was used to sense the operating temperature of the sensor. The output of the thermocouple was connected to a digital

temperature indicator. A gas inlet valve was fitted at one of the ports of the base plate. The required gas concentration inside the static system was achieved by injecting a known volume of test gas using a gas-injecting syringe. A constant voltage was applied to the sensor, and current was measured by a digital pico-ammeter. Air was allowed to pass into the glass dome after every NH₃ gas exposure cycle.

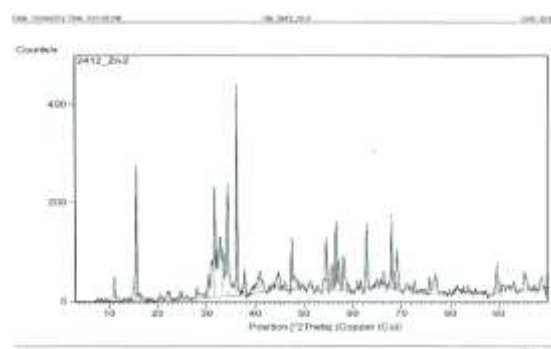
III. MATERIALS CHARACTERIZATION

A. Structural properties (X-Ray Diffractogram)

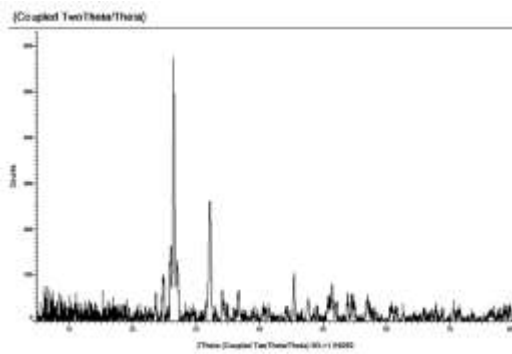
Fig. 2 depicts the XRD patterns of nanostructured ZnO powders within the 2θ range from 0° to 80°. The average crystallite size of the samples were calculated by using Scherer's relation, $t = 0.94 \lambda / \beta \cos\theta$, where, λ is wavelength of X-ray in Å, β is full width at half maximum in radian (FWHM). The observed peaks are matching well with JCPDS reported data of ZnO. Thus the synthesized materials are confirmed. The peaks of the XRD patterns in figure 2 (a) correspond to ZnO, are observed to be amorphous and microcrystalline mixed structures in nature. The average grain size was determined using Scherer's formula and was estimated to be of 12- 20 nm. The crystals show somewhat anisotropy because different directions within the repeating pattern interact differently with incident radiations.



(a) Z_b



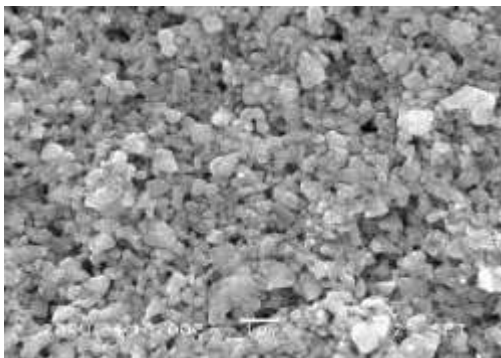
(b) Z₁



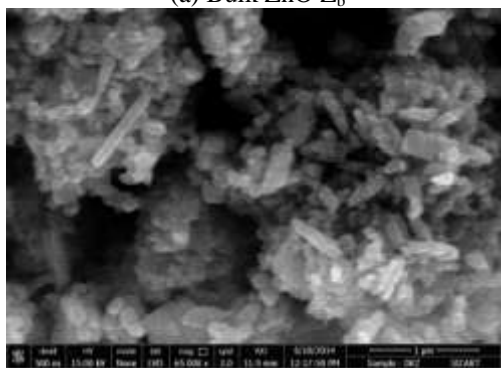
(c) Z₂

Fig.2: XRD of (a) bulk ZnO Z_b, (b) nano-ZnO Z₁ sample, (c) nano-ZnO Z₂ sample

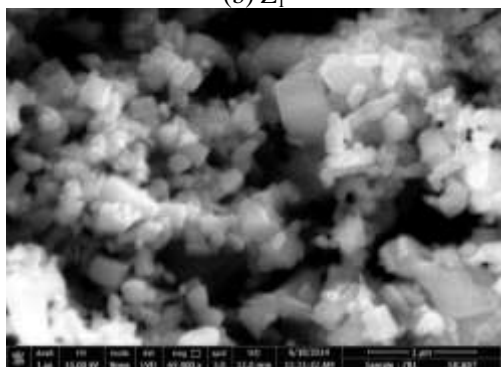
B. Scanning Electron Microscopic Studies (Microstructural analysis)



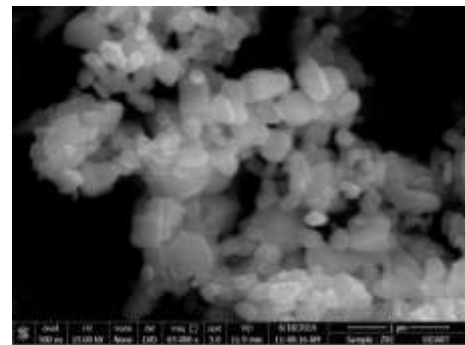
(a) Bulk ZnO Z_b



(b) Z₁



(c) Z₂



(d) Z₃

Fig. 3 SEM images of nanostructured ZnO films

Fig. 3 (a) shows the SEM image of bulk ZnO (Z_b) powder fired at 500°C. The average particle size of the powder was found to be ~ 500 nm with spherical and narrow size distribution. Fig 3 (b) shows the SEM image of nanostructured ZnO (Z₁) thick film consisting of nanorods of ZnO which are distributed randomly. The highest gas response is attributed to the fact of ZnO nanorods formed in the sample powder whose average diameters is about 12 nm, the chemical reactivity of the surface of ZnO increases and adsorbs the moisture on the film at room temperature. On exposure, NH₃ gas reacts with moisture and NH₄OH is formed as a byproduct. The volatility of the byproduct itself explains the quick response and fast recovery of the sensor. Fig. 3 (c and d) show the SEM images of nano ZnO samples (Z₂ and Z₃). The decrease in the gas response of this film is due to the masking of the film by large grains of ZnO and low porosity.

IV. GAS SENSING PERFORMANCE

A. Measurement of gas response, selectivity, response and recovery time

Response of the sensor for the particular gas can be defined as the ratio of the change of conductance of the sample upon exposure to the gas to the conductance in air ambient. The gas response (S) can be written as:

$$\text{Gas response} = \frac{G_g - G_a}{G_a} = \frac{\Delta G}{G_a}$$

where G_a = conductance in air and G_g = conductance in a target gas.

Specificity or selectivity of the sensor can be defined as the ability of a sensor to respond to a particular gas in the mixture of various gases. Response time (RST) is defined as the time required for a sensor to attain the 90% of the maximum increase in conductance after exposure of the test gas, while recovery time (RCT) is the time taken to get back 90% of the maximum conductance [28-35] in air.

B. Sensing performance of the sensor

B (i). Effect of operating temperature

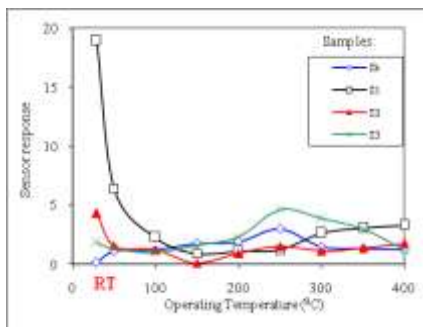


Fig. 4 Variation of gas response with op. temperature

Fig. 4 depicts the variation of NH₃ gas (10 ppm) response with operating temperature. The largest response of Z₁ was observed to be 19 to NH₃ at room temperature. The response of the sensor to ammonia at room temperature is expected to be monitored by adsorption of moisture on the activated ZnO film. The cumulative effect would decrease the film resistance, exhibiting the ammonia response at room temperature. The oxygen adsorption-desorption mechanism is not employed to respond to NH₃ gas at room temperature, as oxygen species are not adsorbed at room temperature. As temperature increases, the moisture from the film surface evaporates and hence the response would decrease further, even up to 400°C.

B (ii). Effect of NH₃ gas concentration

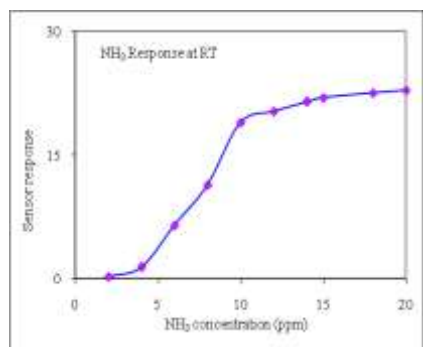


Fig. 5 Variation in response with NH₃ gas concentration (ppm)

The variation of gas response of the Z₁ sample with NH₃ gas concentration at room temperature is represented in Fig. 5. This film was exposed to varying concentrations of NH₃. For the Sensor, the response values were observed to increase continuously with increasing the gas concentration up to 10 ppm at room temperature. The rate of increase in response was relatively larger up to 10 ppm, and smaller during 10 and 20 ppm. The region on the plot below 5 ppm, is called as cutoff region. The region in between 5 to 10 ppm

is called as the active region and above 10 ppm, there is a saturation region. For proper functioning of the sensor, it should be worked in the active region, only. At lower gas concentrations, the unimolecular layer of gas molecules would be formed on the surface of the sensor which could interact more actively giving larger response. The multilayers of gas molecules on the sensor surface, at the higher gas concentrations, would result into saturation in response beyond 10 ppm gas.

B (iii). Effect of Crystallite Size

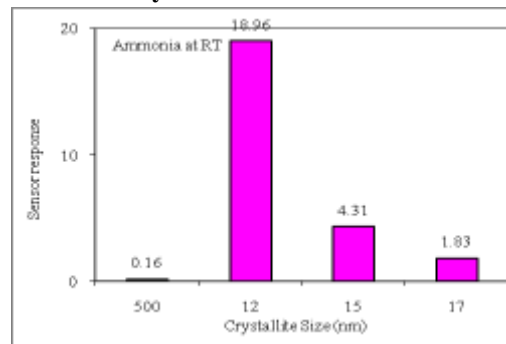


Fig. 6 Variation of gas response with crystallite size (nm)

The response of nano-ZnO films to 10 ppm NH₃, as a function of the crystallite size (nm) is shown in Fig. 6. The sample with a crystallite size / diameter of nanorod of 12 nm was observed to be the most sensitive at room temperature. The higher response of this sample as compared to other samples may be due to the optimum porosity would be created to oxidize the gas on the surface. This leads the decrease in the resistance considerably large, giving larger response.

B (iv). Selectivity to NH₃ against various gases

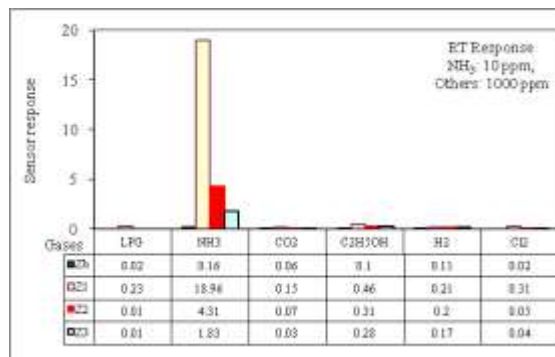


Fig. 7 Selectivity of NH₃ gas among various gases

Fig. 7 depicts the selectivity of the nano-ZnO sensors. The sensors showed high selectivity to NH₃ against LPG, CO₂, C₂H₅OH, H₂, and Cl₂ gases.

V. DISCUSSION

ACKNOWLEDGEMENTS

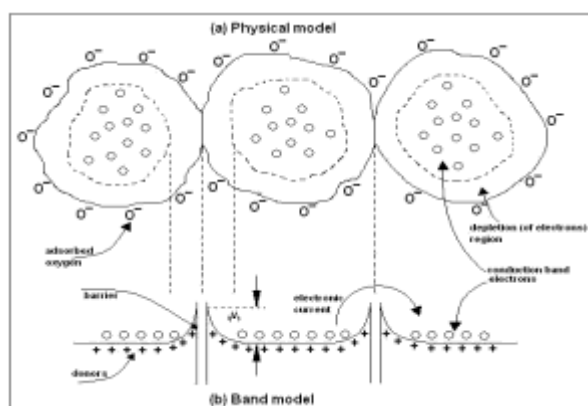
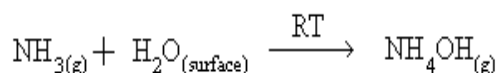


Fig. 8 Mechanism of NH₃ gas sensing

The surface reaction process in Fig. 8 can explain the selective response of the sensing element to ammonia at room temperature. Thick films of nanostructured ZnO consist of an appropriate number of ZnO grains interconnected to each other through boundaries. This attributes to the formation of potential barrier among the grains leading to increase the resistance of the sample, in the absence of the target gas. A few moles of H₂O from air (moisture) could be expected to be adsorbing on the surface of the sensor at room temperature. Upon exposure of ammonia, the resistance of the sensor was decreased, remarkably [21], which may be due to the surface reaction of ammonia with physisorbed H₂O or by proton conductivity via NH₄⁺ cations. The solid acidity on the sensor surface would form NH₄⁺ cations, which constitutes the proton conductivity leading to a crucial decrease of the resistance. This decreases the potential barrier among the nanoscaled ZnO grains.



Ammonium hydroxide (NH₄OH) was produced as a byproduct of this reaction, which is volatile in nature and gets evaporated which explains the recovery of the sensor to its original chemical status.

VI. CONCLUSION

1. Bulk ZnO thick films were observed to be less sensitive to trace level of NH₃ at room temperature.
2. The sensor was found to be highly selective to NH₃ gas (10 ppm) in the mixture of various gases of higher concentrations (1000 ppm).
3. The sensor showed quick response (~ 5 s) and recovery (~ 12 s) to NH₃.

Authors are grateful to Hon'ble Kakasaheb Vasant Rao More, President and Prin. B. V. Patil, Rani Laxmibai College, Parola, Maharashtra, India for providing excellent laboratory facilities, at Bulk and Nanomaterials Research Laboratory, Dept. of Physics, R. L. College, Parola, Dist-Jalgaon, MHS, India.

REFERENCES

- [1]. C. Wagner, J. Chem. Phys. 18 (1950) 69.
- [2]. T. Seiyama, A. Kato, K. Fujiishi, M. Nagatanui, Anal. Chem., 34 (1962) 1502.
- [3]. N. Taguchi, Japanese patent application, 1962.
- [4]. <http://www.figarosensor.com>, available online.
- [5]. M. Kaur, N. Jain, K. Sharma, C. Thinaharan, S. Gupta, J. Yakhmi, proceeds. ISMC-06, BARC, India 2006, pp. 676.
- [6]. R. Rella, Sens. Actuators B 58 (1999) 283-288.
- [7]. M. Ferroni, Sens. Actuators B 58 (1999) 289-294.
- [8]. Y. K. Chung, Sens. Actuators B 60 (1999) 49-56.
- [9]. A. Chiorino, Sens. Actuators B 59 (1999) 203-209.
- [10]. D. R. Patil, L. A. Patil, P. P. Patil, Sens. Actuators B 126 (2007) 368-374.
- [11]. L. R. Narasimhan, W. Goodman, C. Kumar, N. Patel, PNAS. 98 (2001) 4617-4621.
- [12]. R. E. de la Hoz, D. P. Schueter, W. N. Rom, Am. J. Ind. Med. 29 (1996) 209-214.
- [13]. C. M. Leung, C. L. Foo, Ann. Acad. Med. Singapore 21 (1992) 624-629.
- [14]. R. A. Michaels, Environ. Health Perspective, 107 (1999) 617-627.
- [15]. L. G. Close, F. I. Catlin, A. M. Cohn, Arch: Otolaryngol, 106 (1980) 151-158.
- [16]. R. F. Dasmann, Environmental conservation, (4th Ed.) John Wiley and sons, Inc., New York, (1976) 310-338.
- [17]. W. B. Durham, Industrial Pollution, Sax, N.I. (Ed.), Van Nostrand Reinhold Co., New York, (1974) 10-35.
- [18]. D. F. Shriver, P. W. Atkins, Inorg. Chem. (3rd-ed.), Oxford University press; (2004) 184-190.
- [19]. G. S. Sodhi, Fundamental concepts of Environmental Chemistry, (1st edition) Narosa Publishing House New Delhi, (2002) 215-302, 405-427.
- [20]. M. S. Wagh, G. H. Jain, D. R. Patil, S. A. Patil, L. A. Patil, Sens. Actuators B 115 (2006) 128-133.
- [21]. G. S. Trivikrama Rao, D. Tarakarama Rao, Sens. Actuators B 55 (1999) 166-169.
- [22]. D. Mutschall, K. Holzner, E. Obermeier, Sens. Actuators B 36 (1996) 320-324.
- [23]. A. L. Kukla, Y. M. Shirshov, S. A. Piletsky, Sens. Actuators B 37 (1996) 135-140.
- [24]. I. Lahdesmaki, A. Lewenstam, A. Ivaska, Talanta 43 (1996) 125-134.
- [25]. X. Wang, N. Miura, N. Yamazoe, Sens. Actuators B 66 (2000) 74-76.

-
- [26]. C. N. Xu, N. Miura, Y. Ishida, K. Matuda, N. Yamazoe, Sens. Actuators B 65 (2000) 163-165.
 - [27]. Y. D. Wang, X. H. Wu, Q. Su, Y. F. Lee, Z. L. Zhou, Solid-State Electron. 45 (2001) 347-350.
 - [28]. D. R. Patil, L. A. Patil, G. H. Jain, M. S. Wagh, S. A. Patil, Sensors and Transducers 74 (2006) 874.
 - [29]. D. R. Patil, L. A. Patil, Sensors and Transducers 70 (2006) 661.
 - [30]. D. R. Patil, L. A. Patil, Sensors IEEE 7 (2007) 434.
 - [31]. D. R. Patil, L. A. Patil, Sens. Actuators B 123 (2007) 546.
 - [32]. D. R. Patil, L. A. Patil, Sensors and Transducers 81 (2007) 1354.
 - [33]. L. A. Patil, D. R. Patil, Sens. Actuators B 120 (2006) 316.
 - [34]. S. V. Bangale, S. M. Khetre, D. R. Patil, S. R. Bamne, Sens. Transducers 134 (2011) 95-106.
 - [35]. D. R. Patil, L. A. Patil, Sens. Transducers 81 (2007) 1354-1363.